

AFML-TR-76-81
Part II

(2)

DEFECT-PROPERTY RELATIONSHIPS IN COMPOSITE MATERIALS

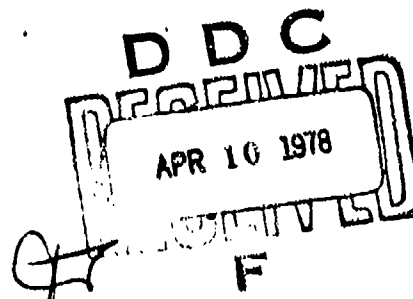
Virginia Polytechnic Institute & State University
Blacksburg, Virginia 24061

June 1977

TECHNICAL REPORT AFML-TR-76-81, Part II

Final Report for Period 3 February 1975 - 3 February 1977

Approved for public release; distribution unlimited.



AIR FORCE MATERIALS LABORATORY
AIR FORCE WRIGHT AERONAUTICAL LABORATORIES
AIR FORCE SYSTEMS COMMAND
WRIGHT-PATTERSON AIR FORCE BASED, OHIO 45433

AD No. _____
DDC FILE COPY

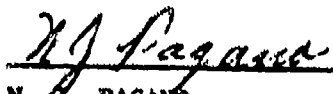
ADA 052358

NOTICE


When Government drawings, specifications, or other data are used for any purpose other than in connection with a definitely related Government procurement operation, the United States Government thereby incurs no responsibility nor any obligation whatsoever; and the fact that the government may have formulated, furnished, or in any way supplied the said drawings, specifications, or other data, is not to be regarded by implication or otherwise as in any manner licensing the holder or any other person or corporation, or conveying any rights or permission to manufacture, use, or sell any patented invention that may in any way be related thereto.

This report has been reviewed by the Information Office (ASD/OIP) and is releasable to the National Technical Information Service (NTIS). At NTIS, it will be releasable to the general public, including foreign nations.

This technical report has been reviewed and is approved for publication.


N. J. PAGANO
Project Engineer

FOR THE DIRECTOR


S. W. TSAI, Chief
Mechanics & Surface Interactions Branch
Nonmetallic Materials Division

Copies of this report should not be returned unless return is required by security considerations, contractual obligations, or notice on a specific document.

AFLC-WPAFB-NOV 74 500

SECURITY CLASSIFICATION OF THIS PAGE (When Data Entered)

REPORT DOCUMENTATION PAGE		READ INSTRUCTIONS BEFORE COMPLETING FORM	
1. REPORT NUMBER AFML-TR-76-81, Part II	2. GOVT ACCESSION NO.	3. RECIPIENT'S CATALOG NUMBER	
4. TITLE (and Subtitle) DEFECT-PROPERTY RELATIONSHIPS IN COMPOSITE MATERIALS. Part II.		5. TYPE OF REPORT & PERIOD COVERED Final Report 3 Feb 75 - 3 Feb 77	
7. AUTHOR(s) (10) K. L. Reifsnider E. G. Henneke W. W. Stinchcomb		8. CONTRACT OR GRANT NUMBER(s) (15) F33615-75-C-5719	
9. PERFORMING ORGANIZATION NAME AND ADDRESS Virginia Polytechnic Institute & State University Engineering Science and Mechanics Department Blacksburg, VA 24061		10. PROGRAM ELEMENT, PROJECT, TASK AREA & WORK UNIT NUMBERS (16) 73403A1 (17) 03	
11. CONTROLLING OFFICE NAME AND ADDRESS Air Force Materials Laboratory, Mechanics and Surface Interactions Branch, Nonmetallic Materials Div., Wright Patterson Air Force Base, Ohio 45433		12. REPORT DATE (17) June 77	
14. MONITORING AGENCY NAME & ADDRESS (if different from Controlling Office)		13. NUMBER OF PAGES 54 (12) 55P	
		15. SECURITY CLASS. (of this report) Unclassified	
16. DISTRIBUTION STATEMENT (of this Report) Approved for public release; distribution unlimited.		18a. DECLASSIFICATION/DOWNGRADING SCHEDULE	
17. DISTRIBUTION STATEMENT (of the abstract entered in Block 20, if different from Report)		F	
18. SUPPLEMENTARY NOTES			
19. KEY WORDS (Continue on reverse side if necessary and identify by block number) Composite Materials, Graphite-epoxy, Defects, Properties, First Ply Failure, Nondestructive Testing, Delamination, Cracking			
20. ABSTRACT (Continue on reverse side if necessary and identify by block number) This report describes the results of an investigation of the nature of damage in two graphite-epoxy laminates under various loading histories, with special attention to the changes in mechanical properties caused by specific damage mechanisms. The results include several new findings, the development of unique investigative methods and some substantial deviations from common model predictions.			

DDC
APR 10 1978
RECEIVED
F

PREFACE

This is the final report on the activities and results of project number 352832-1 titled "Defect-Property Relationships in Composite Materials" recently completed at the Virginia Polytechnic Institute and State University under Contract F33615-75-C-5119 to the Air Force Materials Laboratory, Wright Patterson Air Force Base, Ohio. The technical monitor of the work is Dr. N. J. Pagano. The authors gratefully acknowledge the support of the Materials Laboratory for this program. The investigations were completed between the dates of 3 February, 1975 and 3 February, 1977.

The authors also express their appreciation to Fran Carter for typing the manuscript.

ACCESSION for	
NIS	White Section <input checked="" type="checkbox"/>
DOC	Black Section <input type="checkbox"/>
PLANNING	
U.S.	
DISTRIBUTION AND COPIES	
CPL	
A	

TABLE OF CONTENTS

<u>Section</u>		<u>Page</u>
I.	INTRODUCTION	1
II.	EXPERIMENTAL METHODS	4
	1. Quasi-Static Testing	4
	2. Fatigue Testing	6
	3. Ultrasonic Pulse-Echo Technique	6
	4. Video- and Vibrothermography	9
	5. Microscope Examinations	10
III.	RESULTS	10
	1. Stress-Strain Behavior	10
	2. Stress Distributions	13
	3. Ultrasonic Attenuation - Observations	21
	4. Acoustic Emission Observations	26
	5. Replication Results	32
	6. Preliminary Fatigue Results	34
	7. Sectioning Studies	38
	8. Strain Gage Data	43
IV.	PRINCIPAL FINDINGS & CONCLUSIONS	44
	REFERENCES	48

LIST OF ILLUSTRATIONS

<u>Figure</u>		<u>Page</u>
1.	Schematic of specimen geometry	5
2.	Predicted and observed stress-strain curves	11
3.	Static strength distributions for type I and type II material	14
4.	Axial thermal curing stress distribution across the width for types I and II material	16
5.	Interlaminar normal stresses due to thermal curing	18
6.	Interlaminar normal stresses due to curing stresses plus a 2 kip load - type I material	19
7.	Interlaminar normal stresses due to curing stresses plus a 2 kip load - type II material	20
8.	Attenuation change during quasi-static loading of a type I specimen	23
9.	Ultrasonic attenuation and strain as a function of load level for a type II material	24
10.	Percent change in ultrasonic attenuation compared to the original attenuation plotted as a function of load level	27
11.	Ultimate failure load compared to the load level at which a 5% ultrasonic attenuation change was first reached	28
12.	Acoustic emission during quasi-static loading of type I material	30
13.	Acoustic emission during quasi-static loading of type II material	31
14.	Replica of damage in a type I specimen - edge view	33
15.	Strain gage positions on specimen gage section	42

LIST OF TABLES

<u>Table</u>		<u>Page</u>
I.	Room Temperature Material Property Data for Type AS/3501 Graphite Epoxy	3
II.	Average Mechanical Properties of Graphite Epoxy Unidirectional Laminates	3
III.	Summary of Properties for AS/3501	12
IV.	Thermal Curing Stresses	17
V.	Crack Spacing and Extent of Delamination for Several Load Histories	36

SECTION I

INTRODUCTION

In the field of Science and Engineering, progress can be measured by the degree to which our understandings and descriptions approximate reality. While great sophistication and extreme complexity have been achieved in our efforts to describe the mechanical response of materials, for example, it is still necessary to assume that materials conform to certain "ideal" concepts which form the boundary of our incomplete representation of their behavior. In the special case of composite materials, this situation is further complicated by the fact that these materials are inhomogeneous and nonuniform, and by the fact that they respond anisotropically.

Some very useful models and descriptions of various events which are involved in the development of damage in composite materials have been established. However, the level of understanding (and therefore, reality) involved in these descriptions is sufficiently modest so as to seriously limit their generality and accuracy. Moreover, the improvement of these models and descriptions is hampered by a lack of fundamental information which must be supplied by experimental investigations that specifically address the question of the determination of the precise nature of damage events, rather than simply describing their consequences.

The present investigation addressed this question, i.e., how do defects initiate, how do they grow, and how do they affect the mechanical response of graphite-epoxy (GEP) laminates. More specifically, the objectives were:

1. To identify the precise nature of damage development in quasi-isotropic graphite-epoxy laminates under various load histories,
2. to determine the physical parameters which lead to a loss of strength and/or life,
3. to establish the mechanics of the individual and combined action of these parameters as they influence mechanical response, and
4. to address the question of how these findings can best be described by analysis.

Our approach to these objectives was to investigate the mechanisms of damage in two GEp quasi-isotropic laminates under static and cycled loading using a number of investigative techniques, some of which were developed specifically for this study. In general, the techniques included instrumented tensile and fatigue tests wherein such quantities as stiffness and specific energy dissipation were measured in real time, scanning electron microscope and light microscope studies - under load in some cases, time-resolved thermographic analysis, acoustic emission and ultrasonic attenuation recording, sectioning, and replication investigations. In addition, comparison analysis was carried out including laminate analysis, approximate analysis of edge effects and three-dimensional finite element analysis.

The investigations were carried out on two stacking sequences, a $[0^\circ, \pm 45^\circ, 90^\circ]_s$ laminate hereafter called Type I material, and a $[0^\circ, 90^\circ, \pm 45^\circ]_s$ laminate hereafter called Type II material. The properties of the AS-3501 GEp used to construct these laminates are shown in Table I. The

TABLE 1
ROOM TEMPERATURE MATERIAL PROPERTY DATA
TYPE AS/3501 GRAPHITE EPOXY

Property	Type I ⁽¹⁾	Type II ⁽²⁾
Average 0° Tensile Strength (KSI)	232	225
Average 0° Tensile Modulus (MSI)	20.0	19.4
Fiber Volume (%)	63.8	60.4
Resin Content (%)	28.87	31.95
Density (lb/in. ³)	0.0577	0.0570
Void Content (%)	0.13	0.04
Ply Thickness (in.)	0.0054	0.0054

(1) Panel No. 2206

(2) Panel No. 2506

TABLE 2
AVERAGE MECHANICAL PROPERTIES OF
GRAPHITE EPOXY LAMINATES

Property	Type IA	Type IB	Type II
Elastic Modulus (MSI)	6.6	6.8	6.1
Tensile Strength (KSI)	72.6	65.8	70.5
Fracture Strain (μ in/in)	11,700	10,400	11,400

laminates were supplied by the Hercules corporation in 25 mm by 175 mm specimens with end tabs, as shown in Fig. 1.

SECTION II

EXPERIMENTAL METHODS

As earlier noted, to fulfill the objectives of this study an experimental program was designed to carefully investigate the development of damage in two GrEp laminates subjected to both static and cycled loading. Several new techniques were especially initiated and developed under this effort - vibrothermography, replication and pulse-echo ultrasonic methods. The latter two methods, while not completely new, were modified and developed under this effort to apply to composite materials research. In addition, other techniques were employed to study damage progression: video thermography, x-radiography, light and scanning electron microscopy. These methods have been described earlier in AFML Technical Report No. AFML-TR-76-81. For completeness of this report, these methods are reviewed below with some additional information being given as necessary.

1. Quasi-Static Testing

The quasi-static testing procedures have been detailed in Reference 1. Additional procedures have, however, been initiated during the past year. Several specimens were loaded to intermediate stress values, removed from the machine, sectioned, replaced in the tensile machine, and reloaded to stress values below what was previously obtained. The edges were then scanned optically so that transverse cracks and other damage in the specimens could be noted and counted. More recently,

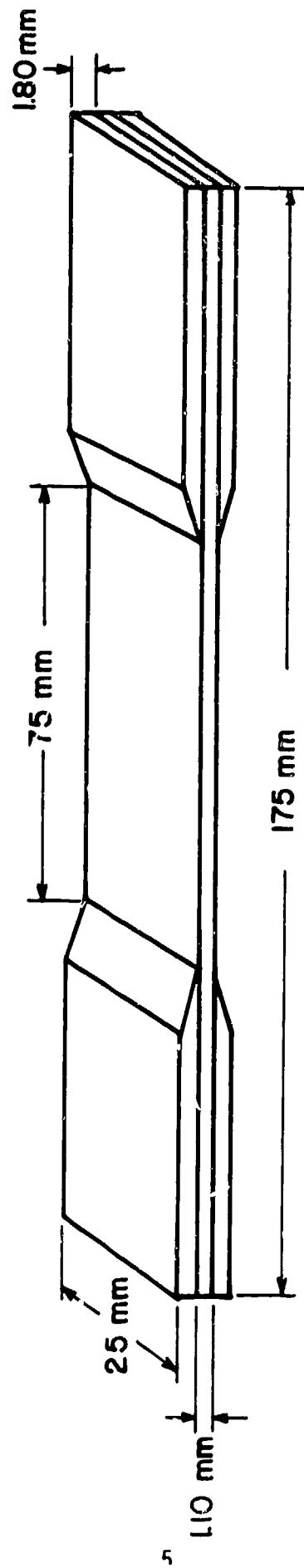


Figure 1. Schematic of specimen geometry

loads have been applied to one specimen in increments, with replicas being made along both edges of the specimen while under constant load. The replicas can then be studied at a latter time to follow the sequence of damage progression along the free edges.

2. Fatigue Testing

The details of this portion of the program have been given in Reference 1 and have remained essentially unchanged during the past year.

3. Ultrasonic Pulse-Echo Technique

The usual definitions and interpretations of data obtained by the ultrasonic pulse-echo technique have been discussed in Reference 1. As discussed there, the attenuation, α , is measured in the laboratory by determining the amplitudes A_1 , A_2 , of any two echoes and by utilizing the relation

$$\alpha = \frac{20}{x_2 - x_1} \log_{10} \frac{A_1}{A_2} \text{ db/unit length} \quad (1)$$

where x_1 and x_2 are the total distances traveled in the material by echo 1 and echo 2, respectively. Note that the two echoes chosen for the amplitude measurement can be any two echoes in the echo train and do not have to be consecutive. The technique used for the measurement of attenuation in this study requires the use of a delay block since the composite specimens are so thin that returning echoes overlap one another on the screen of the cathode-ray tube and can not be individually distinguished. The delay block, when placed on the opposite side of the specimen from the transducer, increases the time of travel of the

ultrasonic stress wave to the point where the echoes are sufficiently separated on the screen that individual amplitude measurements can be made for each echo. Careful analysis [2] of this technique has shown that the use of the delay block requires a re-evaluation of the definition of the attenuation α given above. The experimental value of α is determined by use of the above equation, but the α so calculated does not have the same physical meaning as was used in the derivation of that equation. In deriving the above expression, one assumes that the rate of energy loss from a wave is uniform with distance traveled in the material so that at any point x , the amplitude of the wave is given by

$$A(x) = A_0 e^{-\alpha x} \quad (2)$$

where A_0 is obviously the amplitude at $x = 0$. Then, for the pulse-echo technique, the distance x is normally equal to an integral multiple of twice the length of the specimen, the integral value depending on the number of times the echo has been reflected from the back surface of the specimen. The analysis given in Reference [2] shows that when the delay block is used, any two echoes in the train that is displayed upon the CRT have traveled only twice through the specimen. Thus, ignoring for the moment the addition of any attenuation due to travel in the delay block and transmission and reflection losses which in any case can be accounted for in eqn. (1) by the addition of terms that remain constant during a test, the distances x_1 and x_2 used in eqn. (1) for travel in the specimen are both equal to twice the specimen length, regardless of whether echoes 1 and 2 are consecutive in the train or not. Hence, the denominator in eqn. (1) is zero and the attenuation in the specimen appears as if it can not be determined by simply considering the maximum amplitude of each

echo displayed on the CRT screen. The fact that this was, in fact, done in our technique, requires us to define the value that is measured experimentally as the "effective attenuation".

Actual experimental changes in attenuation have been carefully correlated with damage observed by our other experimental techniques during this study. Hence, it is obvious that the value of α that is calculated using eqn. (1) does have physical relevance to the initiation and progression of the damage state in the specimen even though the value so obtained can not logically be correlated with the definition of α given by eqn. (2). We assert here that we are measuring an "effective" attenuation α using eqn. (1) which does serve as a quantitative measure of the damage state in the specimen. Indeed, we have used observed changes in this attenuation to determine when a quasi-static tension test should be halted so that other observations, such as the sectioning experiments described earlier, could be performed. It is our present contention that the ultrasonic waves interact with the damaged regions in the composite in such a way as to scatter and/or diffract the ultrasonic beam. This causes a beam spread which reduces the amount of ultrasonic energy per unit area of the wave front. As the transducer must always respond to the same wave front area, it sees a returning echo that has been "effectively" attenuated by the beam spread. While such beam spread generally occurs, the original or initial value of attenuation contains this information as well as the losses due to other material and geometric effects. As the attenuation changes with increasing load on the specimen, it becomes apparent that the attenuation changes are responsive to changes in the specimen, i.e., the damaged regions.

The ultrasonic technique used here employed a 1/2" (12.5 mm) diameter

ultrasonic transducer driven at its resonant frequency of 5 MHz. The length of the driving pulse was typically 2-3 μ sec. A Matec pulsed oscillator was employed together with a Matec automatic attenuation recorder to drive and monitor the ultrasonic transducer. The latter instrument electronically performs the calculation of eqn. (1) and outputs an analog signal that is proportional to the determined value of α . The delay block was attached to the opposite side of the specimen from the transducer, the three being held together by a C-clamp. The delay block was made from fused quartz, 1/2" (12.5 mm) diameter x 1" (25 mm) long, with ends polished flat and parallel. The transducer was placed in the middle of the 1" (25 mm) specimen width leaving approximately 1/4" (6.25 mm) on each side between the end of the transducer and the specimen edges.

4. Video- and Vibrothermography

As discussed in Reference 1, the measurement of time-resolved heat emission requires special instrumentation. For this purpose, an AGA 680 video-thermography camera was used to both monitor damage progression during fatigue testing and to study flaws developed by quasi-static loads. In order to observe the latter, it is necessary to put some steady state energy into the specimen. Because of this, a new technique was conceived and is being developed at this laboratory. This new technique, called vibrothermography, utilizes small amplitude, high frequency vibrations to delineate damaged or flawed regions of composites. These vibrations are introduced into the specimen via either a shaker or an ultrasonic cleaning transducer. The specimen is actually clamped at one end to the shaker and allowed to vibrate freely. The thermographic camera is then used to scan the specimen for local hot spots which have

been found to always correspond to a region of damaged material. These hot spots have been found to be quite sensitive to small changes in the frequency of vibration. They can be made to appear or disappear by sweeping through a bandwidth as small as 100-200 HZ.

5. Microscope Examinations

Both optical and scanning electron microscopy were used to follow the initiation and progression of damage along the free edges of the composite laminates. Details of the experimental procedures have been given in Reference 1.

SECTION III

RESULTS

1. Stress-Strain Behavior

The stress-strain curve predicted by laminate theory is plotted in Fig. 2 along with experimental curves for Type I and Type II specimens. The predicted curve was determined using the nominal properties given in Table 3. The knee in the predicted curve is based on a maximum strain to failure criterion applied to the 90° plies and the reduced stiffness in the second portion of the curve is obtained by eliminating the "failed" 90° plies from the laminate analysis. In general, the agreement between the predicted curve and the experimental curves is good. However, the similarities in the stress-strain curves do not imply that the details of defect development and subsequent mechanical response, including fracture, are equally similar.

Laminate theory does not consider the effect of interlaminar stresses on mechanical response; and, therefore, predicts behavior which is independent of the stacking sequence. However, micromechanical observa-

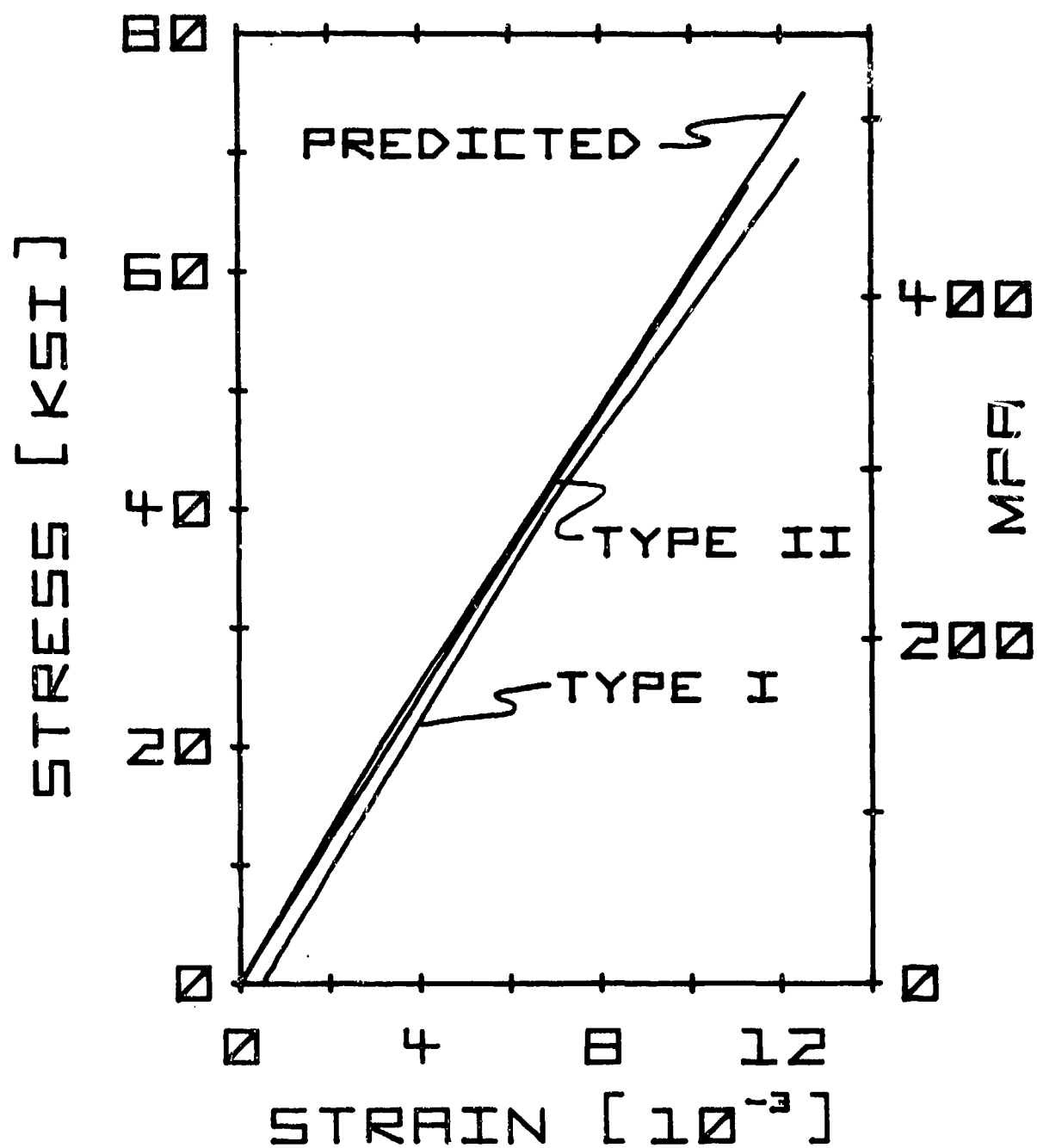


Figure 2. Predicted and observed stress-strain curves

TABLE 3
SUMMARY OF PROPERTIES *
FOR AS-3501

Elastic Stiffness Properties	Tensile Value	Compression Value
E_1	20.2×10^6 psi	17×10^6 psi
E_2	1.4×10^6 psi	1.6×10^6 psi
ν_{12}	0.28	0.28
G_{12}	0.65×10^6 psi	0.65×10^6 psi

Strength Properties

X	235,000 psi	180,000 psi
Y	8,200 psi	25,000 psi
S	17,900 psi	17,900 psi

Other Properties

Thermal expansion coefficients:

α_1 (fiber direction) = -0.2×10^{-6} in/in/°F

α_2 (transverse direction) = 13.0×10^{-6} in/in/°F

Fiber volume fraction 0.62

Ply thickness 0.0052 ± 0.0004 in.

Void content 2%

Density 0.057 lb/in^3

Stress-free temperature 278°F

*Data supplied by Hercules, Inc.

tions of damage details revealed several important differences in response of the two laminates. The first free edge defects to develop under load were transverse cracks in the 90° plies. Due to the two adjacent 90° plies in the center of the Type I specimens, the cracks were twice as long as and opened more than those in Type II specimens. Tensile interlaminar normal stresses in the Type I laminates caused delamination to develop in the 90° plies. In all cases, the delaminations initiated and terminated at transverse cracks and did not grow until the load was increased. Delamination did not develop in the Type II laminates which had compressive interlaminar normal stresses.

Stacking sequence affects not only the size and type of defects which develop under tensile loading but also the strength of the material. The Type I laminates, with longer transverse cracks and delaminations, had generally lower static strengths. The distribution of static tensile strengths is shown in Fig. 3. The mean strength of Type I material is 71.5 ± 4.6 KSI (318.2 ± 20.5 KN) compared to a mean strength of Type II material of 82 ± 3.8 KSI (365 ± 16.9 KN). This represents a difference of 14.6 percent due to stacking. The same ordering of compressive strengths would not be expected however. Compressive loading changes the sign of the interlaminar normal stresses causing delamination and reduced stiffness in the Type II laminates leading to buckling failures.

2. Stress Distributions

A stress analysis of the Type I and Type II materials was performed using both laminated plate theory and a finite element model (3). Each analysis included thermal curing stresses and the in-plane lamination theory results were used to approximate the interlaminar normal stresses at the free edge (4).

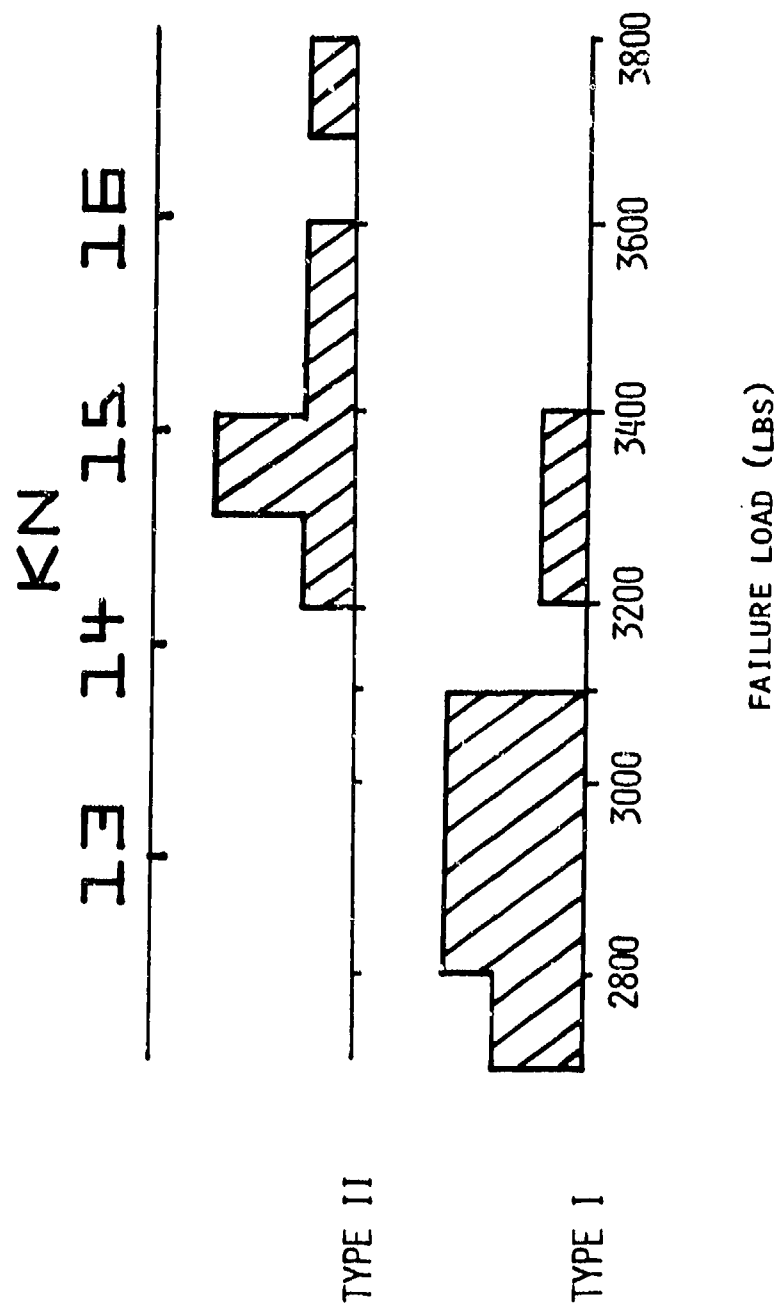


Figure 3. Static strength distributions for Type I and Type II material

The through the thickness distribution of the axial thermal curing stresses σ_x^T in each of the two laminates is shown in Fig. 4. The tensile thermal stress of 4.77 KSI in the 90° layers is approximately 58 percent of the transverse strength of unidirectional material. The in-plane curing stresses at room temperature are given in Table 4. Using the stresses in the 90° plies in the Tsai-Hill failure theory predicts that the strength of these plies must be greater than 4.77 KSI if the thermal stresses are not to cause 90° ply failure. Although this number is about 48 percent less than the reported value of transverse strength (8.2 KSI), the scatter in strength data for 90° tension tests is large enough that some specimens would be expected to have strengths less than 4.77 KSI. It is highly possible then that although the curing stresses are less than those required to cause 90° ply failure in "average" material, some initial cracks due to thermal stresses develop in specimens with weak 90° plies. We have, in fact, observed initial transverse free edge cracks in the 90° plies using the replication technique described in another section.

The approximate through the width distribution of the interlaminar normal stress in the two laminates is shown in Figs. 5 through 7. The interlaminar normal curing stresses at the free edge are tensile in both cases with the largest value in Type I material being approximately three times greater than the largest stress in Type II material. No initial edge delaminations were observed in either type of laminate. The application of a mechanical load in the axial direction increases the tensile interlaminar normal stress in Type I laminates and causes interlaminar compressive stress in Type II laminates. At an applied load of 2 KIPS (331 MPa), the thermal curing stress component is about 21

AXIAL THERMAL CURING STRESS

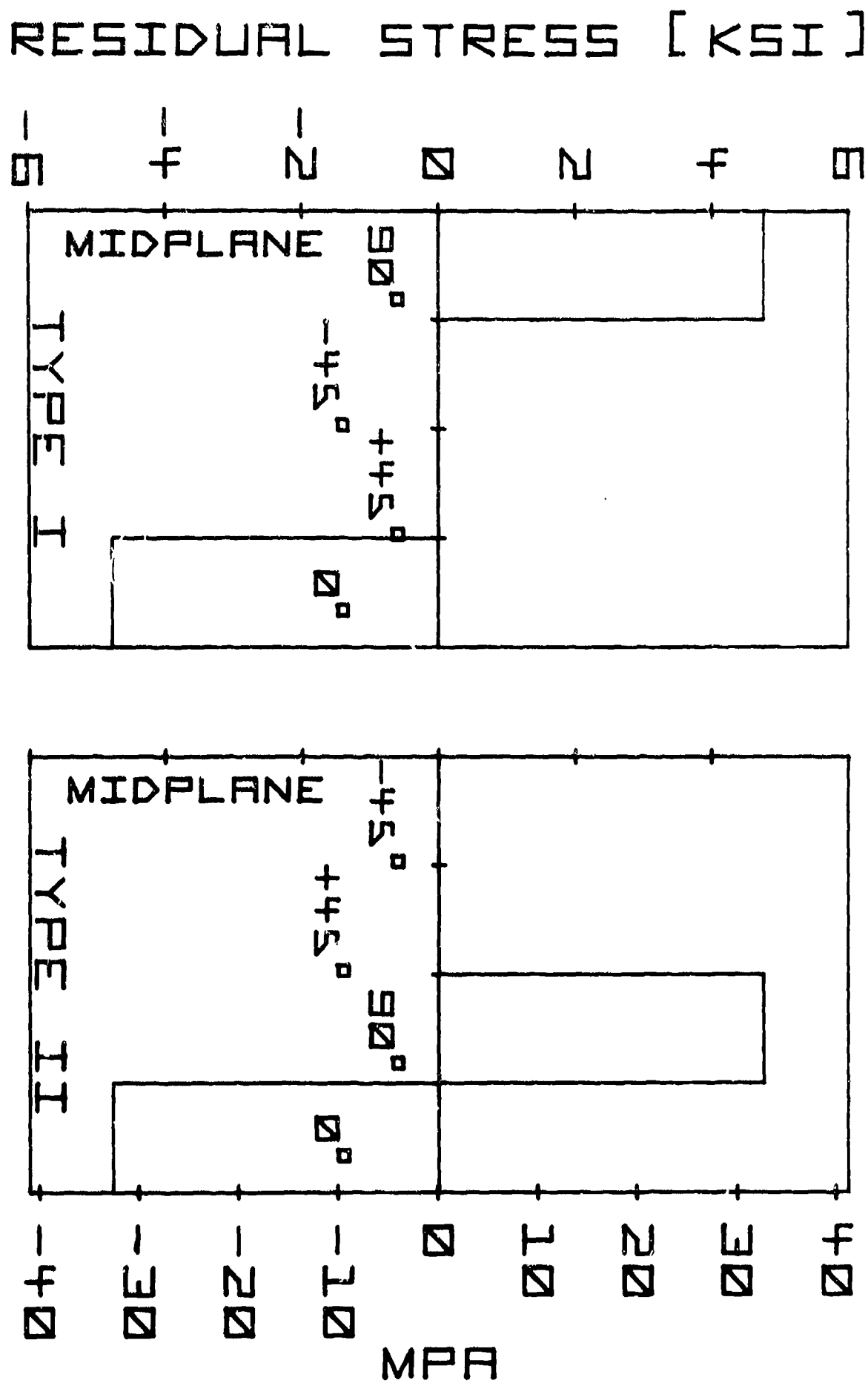


Figure 4. Axial thermal curing stress distribution across the width for Types I and II material

TABLE 4. Thermal Curing Stresses
(Stresses in KSI)

LAMINATE	PLY	σ_x^T	σ_y^T	τ_{xy}^T
Type I	0	-4.77	+4.77	0
	+45	0	0	-4.77
	-45	0	0	+4.77
	90	+4.77	-4.77	0
Type II	0	-4.77	+4.77	0
	90	+4.77	-4.77	0
	+45	0	0	-4.77
	-45	0	0	+4.77

Z STRESS [KSI]

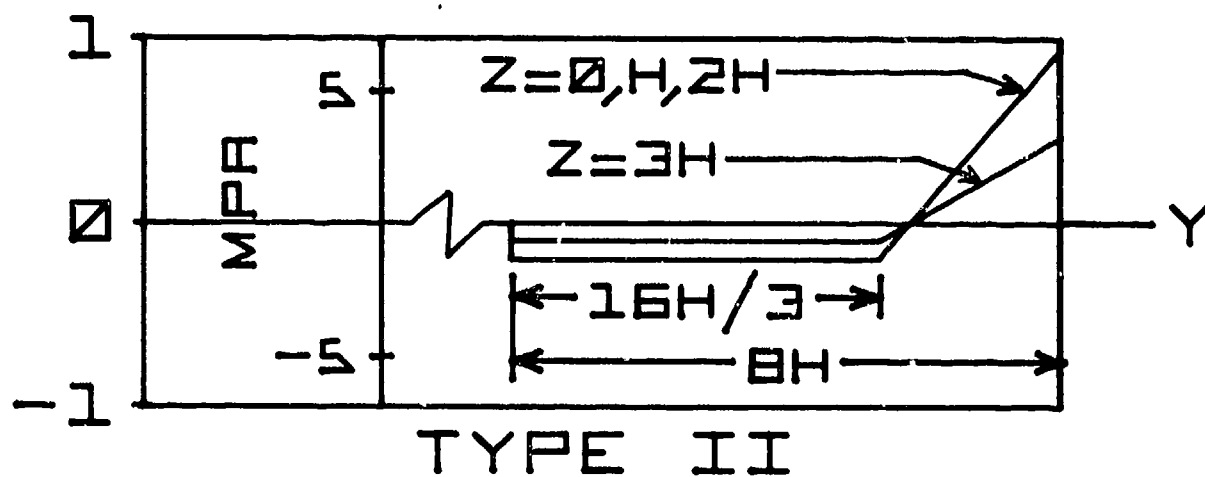
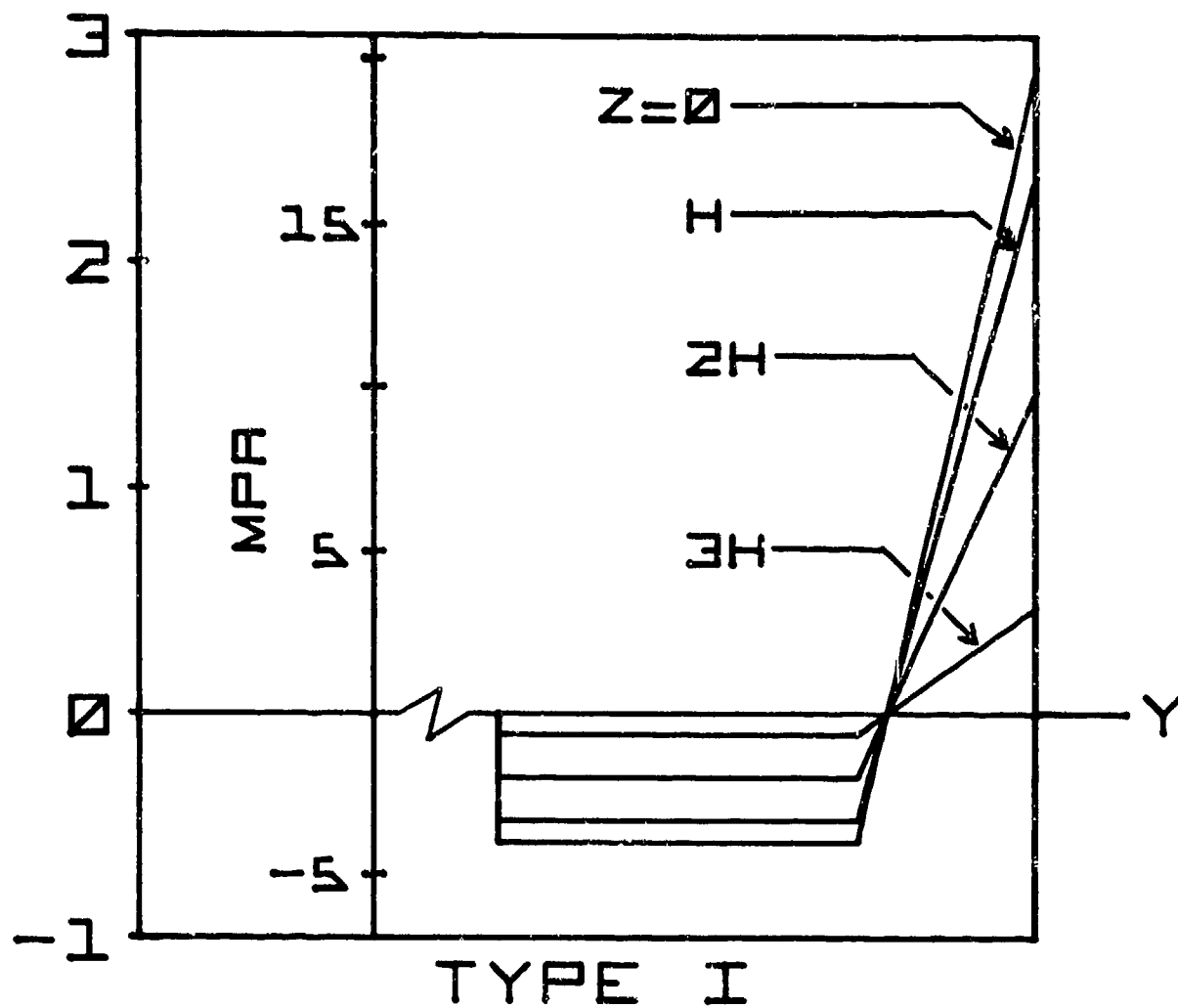


Figure 5. Interlaminar normal stresses due to thermal curing

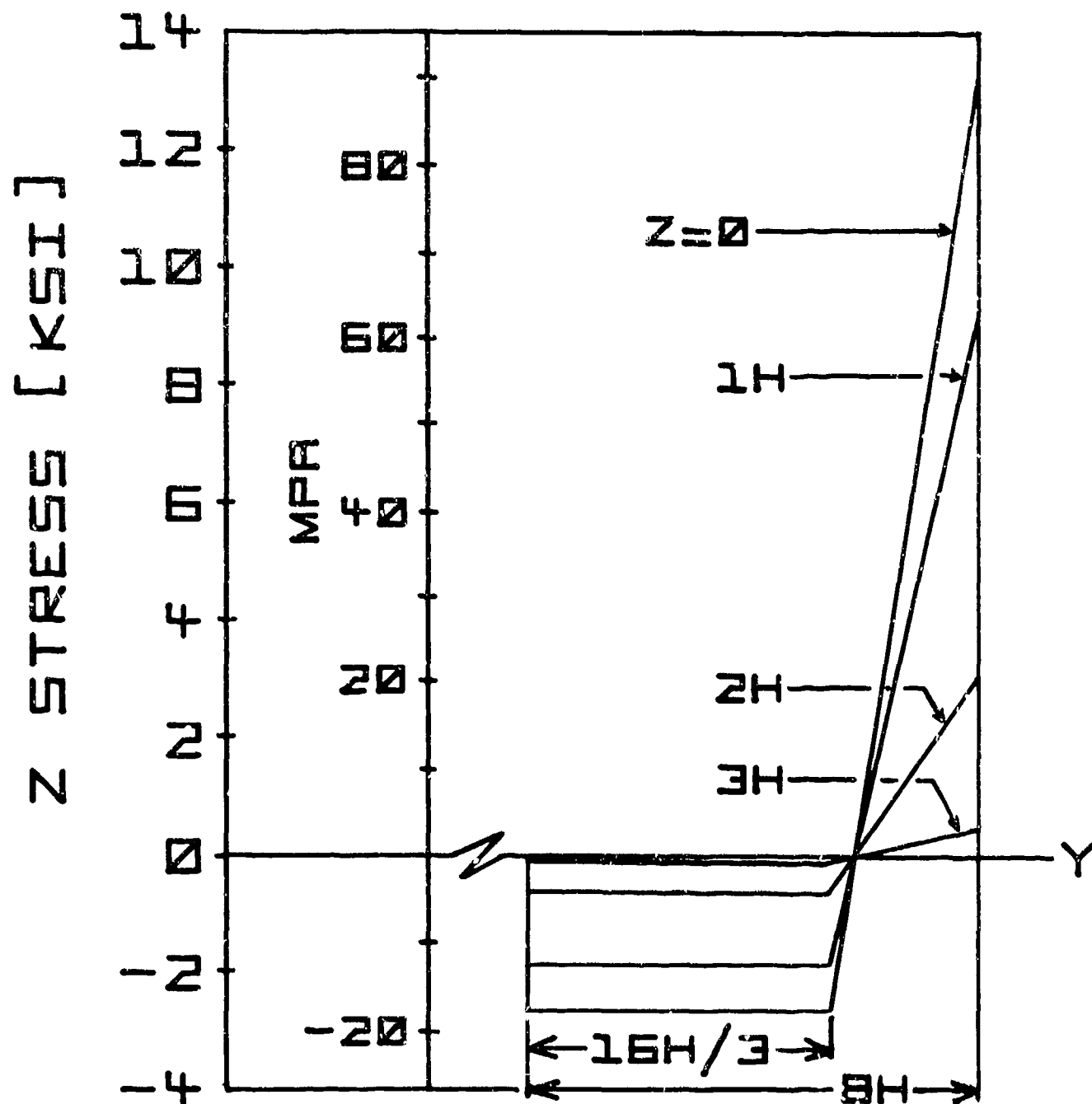


Figure 6. Interlaminar normal stresses due to curing stresses plus a 2 kip load - Type I material

Z STRESS [KSI]

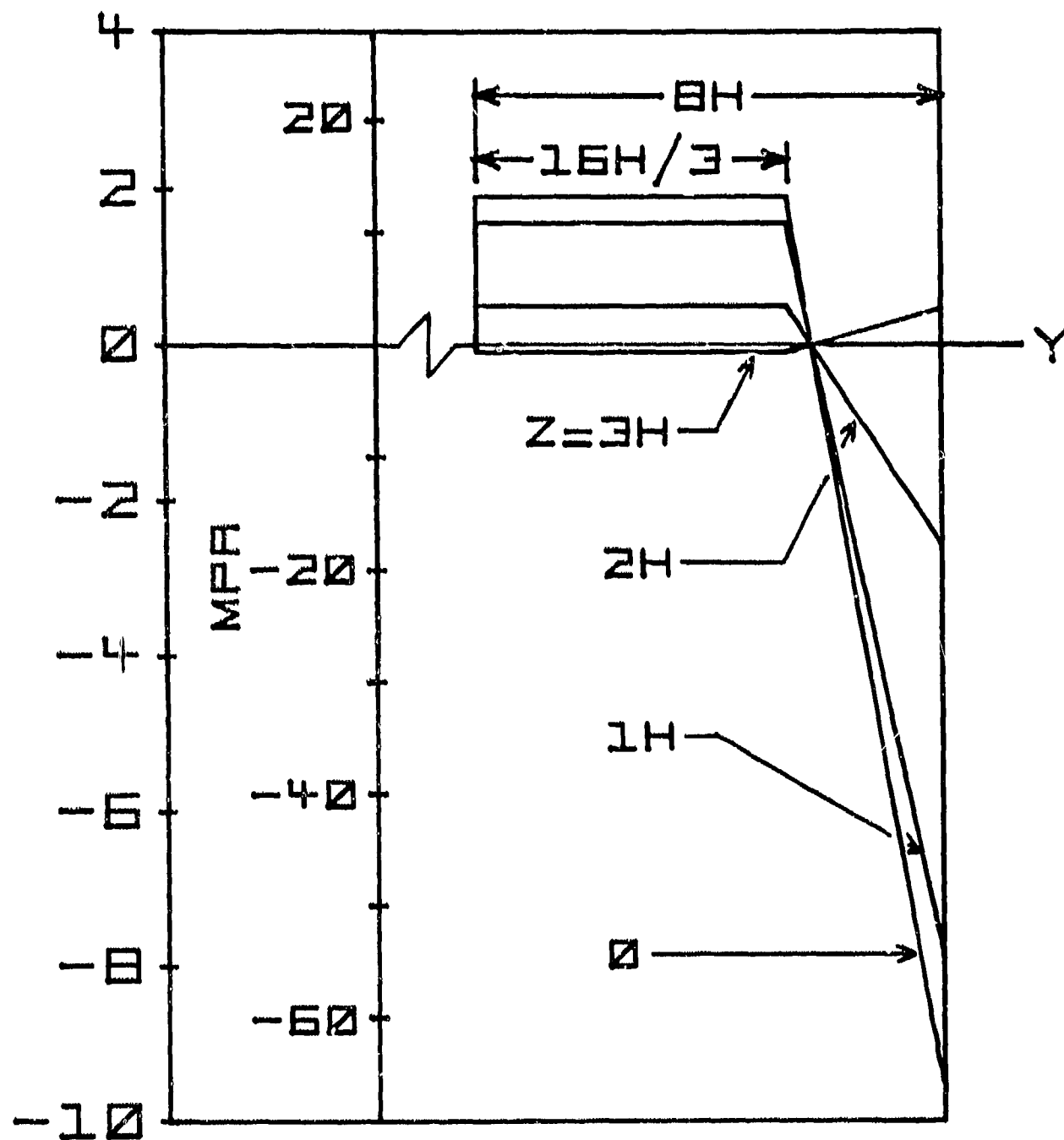


Figure 7. Interlaminar normal stresses due to curing stresses plus a 2 kip load - Type II material

percent of the total interlaminar normal stress at the midplane of the type I laminate.

The values of stress given by laminated plate theory and the interlaminar normal stress approximation were compared with the results of a finite element model. The agreement was generally within two percent and the maximum difference was less than ten percent. Although the finite element model did not give the interlaminar normal stress at the free edge of the specimen, the stress of 3.75 KSI (25.9 MPa) at a distance of 0.0083 (0.21 mm) inches from the free edge agrees very well with the approximate value of 3.8 KSI (26.2 MPa) at the same point for an applied load of 2000 lbs. (8.9 KN) on a type I specimen. The width of the tensile normal stress zone at the free edge is only slightly greater than two ply thicknesses.

3. Ultrasonic Attenuation - Observations

As described in the experimental section, several types of non-destructive test techniques were employed to study the initiation and progression of damage in the composite specimens during various load histories. One of the objectives of this project was to determine which NDE techniques might be most appropriate for this study and to develop them as needed. The ultrasonic pulse-echo method, acoustic emission monitoring, vibrothermography, and visual observation of edge damage by both optical microscope and the replication method have all yielded valuable information pertaining to the initiation and progression of damage. Several of these techniques, while not original to the present authors, have been modified and adopted in novel ways to the study of composite materials. Some particular results obtained through their application to type I specimens are detailed below.

Figure 8 is a typical result for a Type I B specimen [1] for the attenuation of an ultrasonic pulse as a function of applied load during a quasi-static tension test. The most obvious and interesting attribute of the attenuation curve is the sharp rise in attenuation beginning at approximately 1800 lbs. (8.0 KN). This value of load corresponds very closely to the load at the observed knee of the stress-strain curve. For all tests that were run (7), there was a quite evident change in attenuation at the vicinity of the stress-strain knee. In most cases, the attenuation increased at this point, however in two cases, the attenuation decreased. The attenuation is expected to increase since the increasing size of damaged regions with load should serve to scatter ever increasing amounts of the ultrasonic pulse and lead to the apparent attenuation discussed in the experimental section. It is not clear at this point, how one might account for the anomalous behavior of the two specimens. One of these specimens had a sharp drop in attenuation at approximately 1800 lbs. (8.0 KN) and the attenuation remained low until failure. The second had a drop at approximately 1700 lbs. (7.56 KN), and continued to rise and fall until a sharp steady rise occurred 100 lbs. (445 KN) before failure. The ultrasonic pulse-echo method employed here appears to offer very good potential for studying the kind of composite materials used in this study. It is very sensitive to the damage mechanism responsible for the decrease in material stiffness at the knee of the stress strain curve. Obviously, work needs to be done to allow correct interpretation of the data.

A typical real-time attenuation curve for an ultrasonic pulse in a Type II specimen is shown in Figure 9. For comparison purposes, the strain-load curve for the same specimen is also given. Again, as for

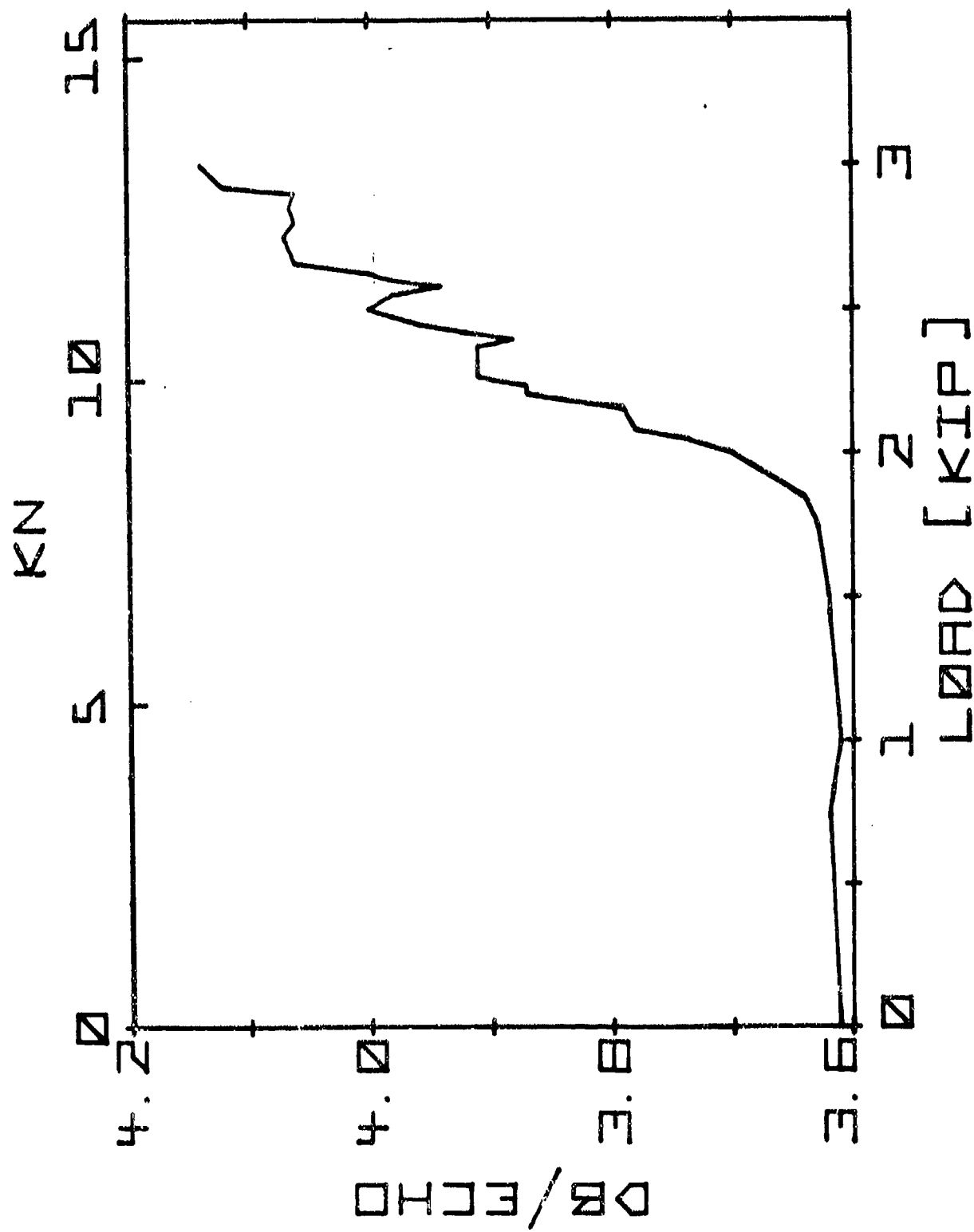


Figure 8. Attenuation change during quasi-static loading of a Type I specimen

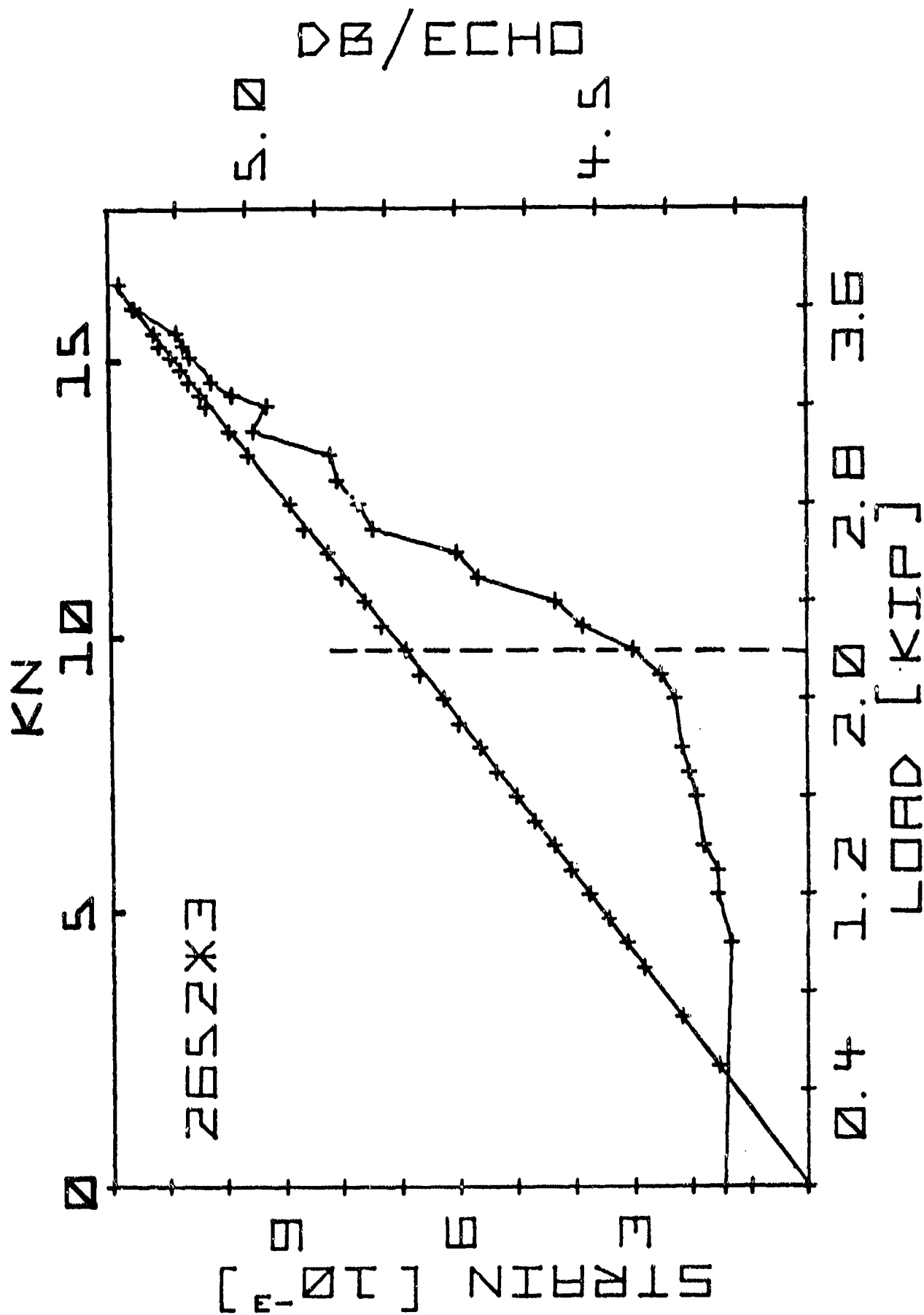


Figure 9. Ultrasonic attenuation and strain as a function of load level for a Type II material

the Type I material, a major rise in attenuation occurs in the vicinity of the knee of the strain-load curve, as indicated by the vertical dotted line. There is also a slight rise in attenuation at approximately 1000 lbs. (4.45 KN). The change in attenuation at this point is more apparent when one looks at the raw data chart than when one plots a number of discrete points as in Figure 9. This rise in attenuation has been tentatively associated with the onset of transverse cracking in the 90° layers, at least through the width of the specimen so that the ultrasonic transducer can respond to the presence of these cracks. This small rise in attenuation has been utilized in one of our sectioning studies to indicate when to end loading. That is, loading was ended just after the rise in attenuation occurred, the specimen was removed from the testing machine and cut axially along the midplane. Optical observations were then made to count the transverse cracks along the edge of the midplane. A larger number of transverse cracks were observed in a specimen loaded to a point above that corresponding to the attenuation rise than in a specimen loaded to a value before any attenuation changes were observed.

The absolute value of attenuation and attenuation changes vary considerably from specimen to specimen. The absolute value is dependent upon such variables as bond, tuning frequency, pulse width, etc. Typically, the instrumentation is tuned to obtain the best signal on the CRT for that particular test. As a result, the absolute value of attenuation has no correlation from specimen to specimen. The total change in attenuation will depend upon specimen variables and the exact nature of the development of damage in the region directly below the transducer. Thus in order to better compare the results for two or more specimens, a relative

change in attenuation can be calculated and plotted versus load. Figure 10 is the percent change in attenuation compared to the original attenuation plotted as a function of load on the material for two type II specimens. Similar results are obtained for the two specimens as can be seen on this graph.

It was further desired to determine if the percent change in attenuation might be utilized to indicate ultimate failure loads. As a starting point in obtaining an answer to this question, a series of plots such as in Figure 10 were made for all specimens tested using the pulse-echo method. From these plots, the value of load for which a five percent increase in attenuation occurred was determined and plotted versus the failure load for that specimen. The results of this determination are given in Figure 11. As can be seen there is a reasonable correlation between these values - the lower the load at which a five percent attenuation occurs, the lower the failure load for that specimen. It should be noted that the 5% change in attenuation was arbitrarily chosen. It was desired to have a small enough value for attenuation change that would give a reasonably early indication of ultimate failure load. Obviously such correlations as shown in Figure 11 will depend upon the specific value chosen for this parameter. However, initial damage occurring early in the 90° layers might be expected to affect the ultimate strength because early first ply failure would lead to the earlier progression of damage into the adjacent plies. Additional work will be performed to better define the selected value of percent attenuation change to correlate with ultimate load.

4. Acoustic Emission Observations

Acoustic emissions were monitored for several type I specimens

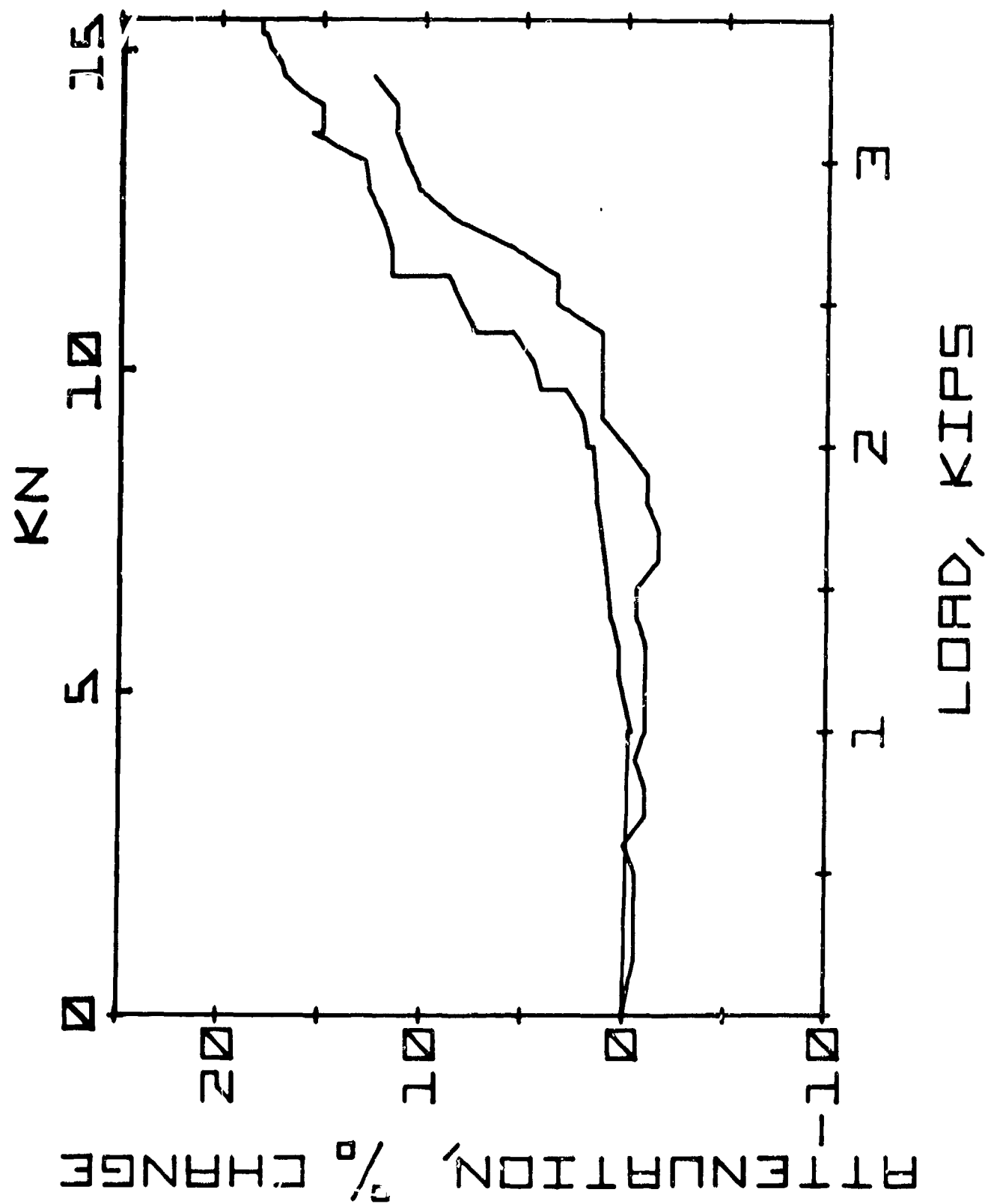


Figure 10. Percent change in ultrasonic attenuation compared to the original attenuation plotted as a function of load level

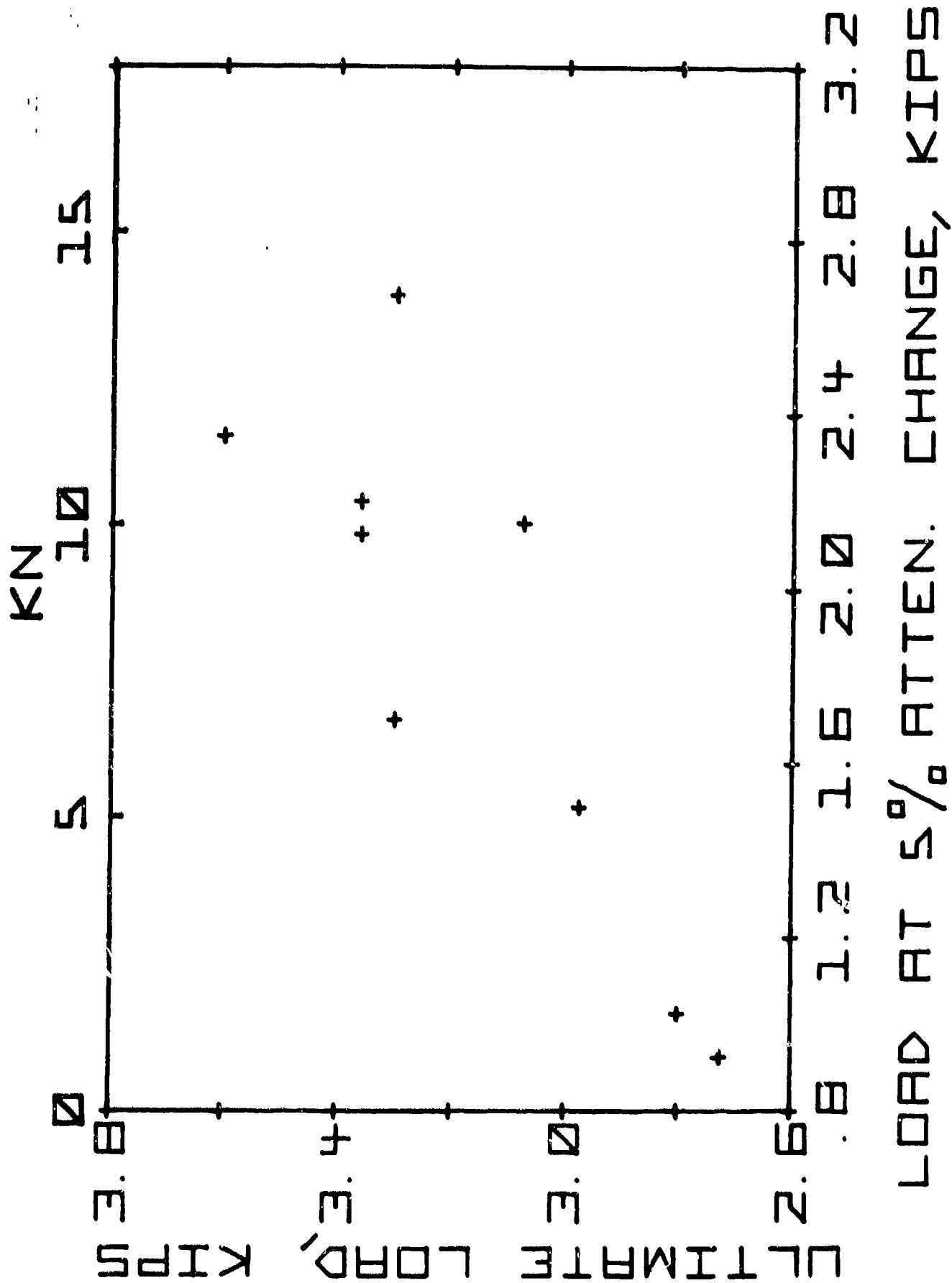


Figure 11. Ultimate failure load compared to the load level at which a 5% ultrasonic attenuation change was first reached

during quasi-static loading. Typical results are given in Figures 12 and 13. In both figures, the total acoustic emission counts are given as a function of applied load. These curves are of a very familiar type, similar results having appeared in many papers and reports. One of the major difficulties with the acoustic emission technique at present is the interpretation of the data gained. Everyone is reasonably convinced that the acoustic emissions are evidence of the development of damage, but just what kind of damage, and what effect this damage has on the remaining strength of the material is undetermined. The AE count curves in Figures 12 and 13 yield, if taken by themselves, provide little new knowledge concerning the progression of damage in the Type I specimens. However, combined with the observations made with the ultrasonic pulse-echo method and by visual examination of the free edge, these figures can be seen to contain corroborating evidence of the progressive stages of damage in the Type I specimen. Figure 12, for example, can be seen to contain three rather distinct regions. Between the onset of countable acoustic emissions and approximately 2100 lbs. (9.34 KN), the total acoustic emission counts increase monotonically by what appears to be an exponential curve. Around 9.34 KN, there is a sudden increase in the rate of acoustic emissions resulting in a very nearly linear rise of the total counts curve until approximately 2700 lbs. (12.0 KN); at which time the rate of emissions decrease slightly and a third distinct region, again having nearly a linear slope with a value less than that of the second region, can be seen. Similar results can be seen in Figure 13. Here there is again a distinct difference in the curve at approximately 2000 lbs. (8.9 KN); however, the third region, if it exists, is not nearly so recognizable. Again, it can be pointed out that the knee of

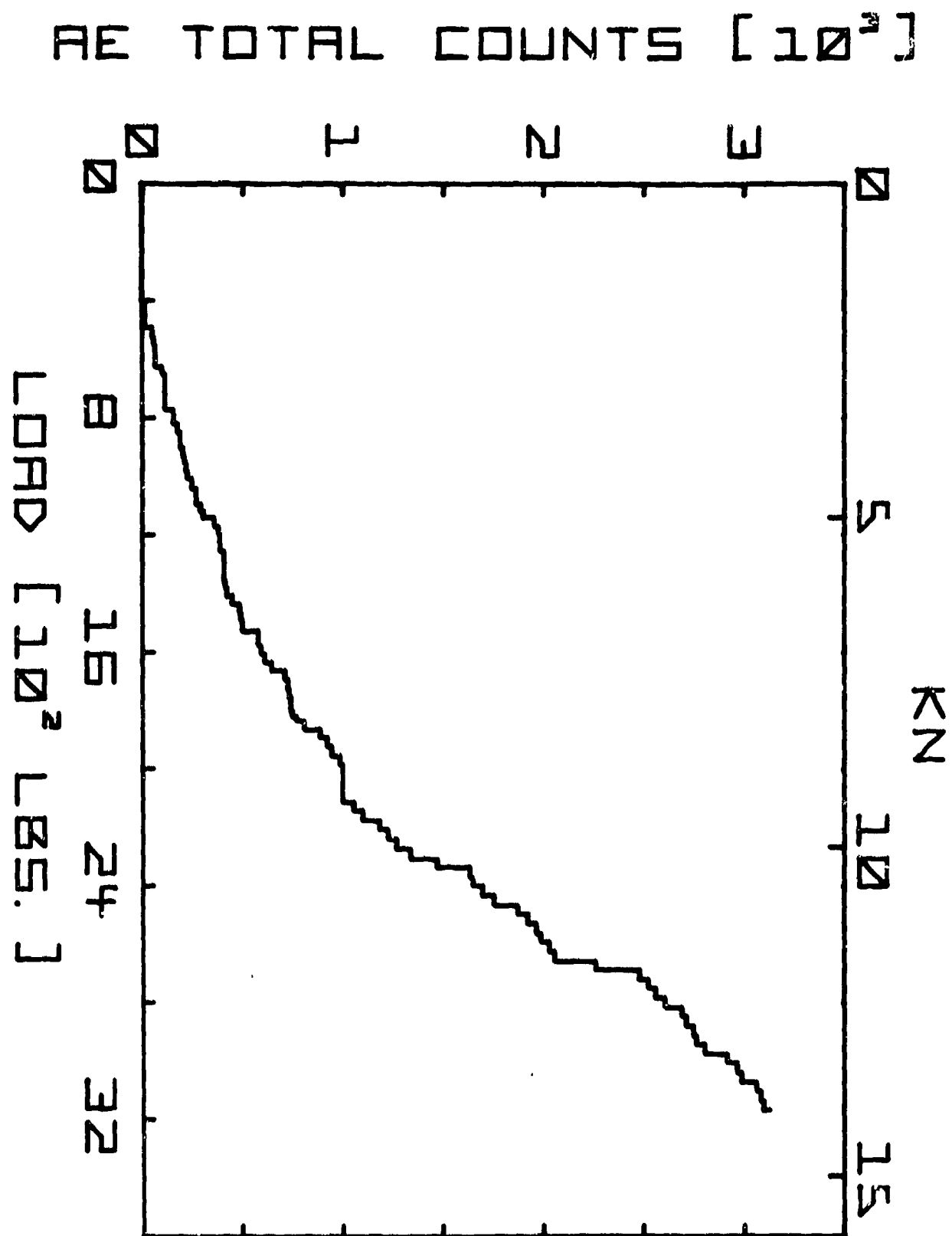


Figure 12. Acoustic emission during quasi-static loading of Type I material

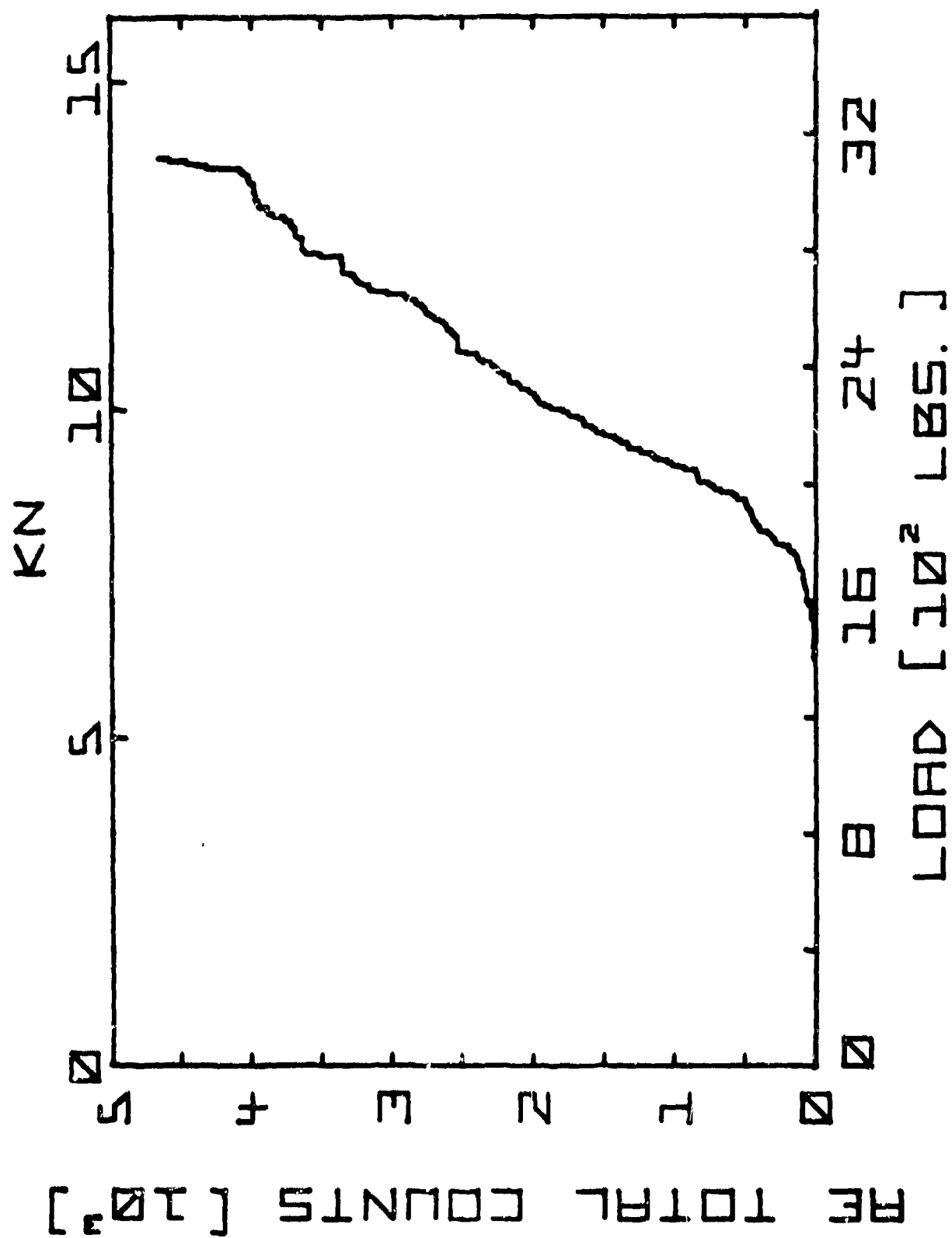


Figure 13. Acoustic emission during quasi-static loading of Type II material

the stress-strain curve for Type I specimens has been found to be in the vicinity of 2000 lbs. (9.8 KN).

5. Replication Results

Several methods of viewing and recording the details of edge damage in the specimens have been used in the present investigation. These include at-load microscopy using a microscope mounted on the crosshead of the testing machine, microscopy using a bench metallograph, scanning electron microscopy, and video studies using video tape apparatus. Each of these methods provided some information on damage development but none gave a complete record of the damage in the specimen at a particular instant in the loading history. Replication has been employed for some time in transmission electron microscopy and fractography to make images of surface details. This technique was modified to provide a record of the damage on the entire edge of the specimen at a particular load level during a tension test or at a particular number of cycles during a fatigue test. By observing the replicas in the order in which they were made, the chronology of defect initiation, growth, and interaction on both edges of the specimen could be studied simultaneously.

The replicas were made by pressing cellulose acetate tape softened with acetone against both edges of the specimen while mounted in the testing machine and under load. After a few minutes, the tape was carefully peeled off the specimen, mounted on a glass slide, and checked for clarity before resuming the test. The replica could then be mounted in a microscope for study or placed in a photographic enlarger to make photographs of selected damage areas such as those shown in Fig. 14. The replica provided a permanent record of the details of damage at a particular instant in the loading history which could be reexamined



Figure 11. Edge view of Type 1 specimen - edge view

whenever needed. In many cases, photographs of each section of the edge of the specimen were assembled to make a montage of the damage along the entire test section. The enlargements, approximately nine feet in length, were laid side by side so that the history of a particular crack or delamination could be traced from the beginning of the test up to fracture. No special preparation to the edge of the specimen is necessary although the resolution of defect details is enhanced by polishing the edge of the specimen. A slurry of micron diamond polishing powder and water applied to a cloth covered polishing wheel gave very good results.

6. Preliminary Fatigue Results

Several specimens of each laminate have been cyclically loaded at maximum loads of 1600 lbs. (7117 N), 2000 lbs. (8896 N), and 2700 lbs. (12010 N), at a stress ratio of $R=0.1$ and a frequency of 1 HZ. These loads produce stresses which are below, near, and above the knee in the static stress-strain curve. Transverse cracks in the 90° plies due to static loading of both laminates generally appear between 1500 lbs. (6672 N) and 2000 lbs. (8896 N) although some cracks have been observed at loads as low as 1000 lbs. (4448 N). Each specimen was statically loaded to the maximum cyclic load and held at that load while replicas of the edges were made. The first cycle was then completed by unloading the specimen. Subsequent load controlled cycles were uniformly and continuously applied except for program interruptions at 50, 100, 500 and 10,000 cycles to make replicas of the edges of the specimen. All replicas were made while the specimen was under a load equal to the maximum cyclic load. Those specimens which survived 10,000 cycles were

loaded to failure and replicas of the edge of the fractured specimen were made. Table 5 contains data for the mean spacing of transverse cracks and extent of delamination for each laminate and load history. Except as noted, the data was obtained from replicas made over the entire three inch gage section of the specimens. The pertinent damage details are summarized below.

A. Type I $[0^\circ, \pm 45^\circ, 90^\circ]_s$

1. Static Preload:

- transverse cracks in 90° plies in all cases.
- local delamination at 1600# and 2000#.
- large delaminations at 2700#.
- the amount of crack branching into -45° plies increased slightly with magnitude of the preload.
- some delamination in $\pm 45^\circ$ interface noted at 2700#.

2. Cyclic Loads:

- number of transverse cracks increased during first 50 cycles at 1600# and 2000#.
- delaminations lengthened.
- the transverse cracks in the -45° plies had extended into the $\pm 45^\circ$ interface causing small delaminations.
- after 500 cycles at 2700#, the delamination had run along the entire specimen length.
- number of transverse cracks in 90° plies at 2700# did not increase between preload and 500 cycles.
- after 10,000 cycles at 1600#, the 90° plies had delaminated along 90% of the edge of the specimen, but the $\pm 45^\circ$ delaminations appeared to increase slightly in length.
- after 10,000 cycles at 2000#, the 90° plies had delaminated

TABLE 5

CRACK SPACING AND EXTENT OF DELAMINATION FOR SEVERAL LOAD HISTORIES

Cycles	Max Load	Type I			Type II		
		90° (avg.*)	Crack Spacing (in.) -45° (avg.*)	+45° (avg.*)	% Delamination 90° ±45°** plies interface	Crack Spacing (in.) 90° (avg.*) +45° (avg.*)	-45° +45°** interface
1/2 (Preload)	1600	0.050	0.121	0.377	28	0.104	a.
	2000	0.182	a.	a.	<1	0.062	0.127
	2700	0.038	0.080	a.	71	0.017	0.401
50	1600	0.042	0.103	0.165	46	0.133	a.
	2000	0.049	0.134	a.	40	0.013	0.046
	2700	0.038	0.080	a.	92	0.013 ^c	0.029 ^c
500	1600	x	x	x	x	x	x
	2000	0.043	0.078	a.	71	x	x
	2700	0.038	0.045	0.201	100	0.014 ^c	0.023 ^c
10,000	1600	0.035	0.069	0.182	91	0.071	a.
	2000	0.036	0.059	0.106	95	0.013	0.151
	2700 ^b						

* average spacing for two plies

** includes both ±45° interfaces

a. insignificant damage

b. 2700 lb. tests terminated after 500 cycles

c. data obtained from a partial replica

x. replica not developed

along 95% of the edge of the specimen, some extension of the $\pm 45^\circ$ delamination noted, small increase in number of transverse cracks in 90° plies between 500 and 10,000 cycles.

B. Type II $[0^\circ, 90^\circ, \pm 45^\circ]_s$

1. Static Preload:

- scattered and irregularly spaced transverse cracks in 90° plies at 1600# and 2000#.
- a regular spacing of approximately $3/8$ the specimen width observed at 2700#.
- some branching of transverse cracks into $+45^\circ$ plies at 2000#.
- widespread branching of transverse cracks into $+45^\circ$ plies (some extending into -45° plies) at 2700#.
- some short longitudinal cracks in 90° plies near tabs at both 2000# and 2700#.

2. Cyclic Loads:

- number of transverse cracks increased during first 50 cycles at 1600# and 2000#.
- at 2000#, 90° cracks extended into $+45^\circ$ plies and some transverse cracks extended into -45° plies after 50 cycles.
- local delamination of $\pm 45^\circ$ interface observed after 50 cycles at 2700#.
- the number of transverse cracks had increased after 10,000 cycles at 1600#.
- number of transverse cracks after 10,000 cycles at 2000# approximately same as number after 50 cycles.
- some delamination of $\pm 45^\circ$ interface after 10,000 cycles at 2000#.

- after 10,000 cycles at 2000#, an irregular transverse crack extended completely across the interior six plies.

The details of the fracture surfaces from the residual strength tests were similar for the two laminates. In each case, two transverse fractures through the outside plies were joined to a transverse fracture in the center by longitudinal separation of the $+45^\circ/-45^\circ$ interface. In Type I material, the outer transverse fractures were through to 0° and $+45^\circ$ plies and the inner fracture was through the -45° , 90° , 90° , -45° plies. For Type II specimens, the outer fractures went through the 0° , 90° , and $+45^\circ$ plies and the inner fracture was through the center -45° plies. Although several 2700# tests failed to reach 10,000 cycles, the residual strength values of the surviving specimens were within the distribution of static values shown in Figure 3.

7. Sectioning Studies

In order to supplement the data regarding crack growth obtained from the nondestructive testing techniques, we performed a series of destructive tests whereby we cut, or sectioned, several specimens along a longitudinal line through the center of their width. After the sectioning the two new edges which were in the interior of the specimen were studied to determine the nature of any flaws intersected by the cut. Since a limited number of such tests was possible within the constraints of the program, the results of several individual examinations will be indicated below.

First, it is interesting to note that some cracks were found in the control specimens which were sectioned without any test load application, i.e., in the as-received condition. These cracks were very small, difficult to find, and small in number - ten or less on a given specimen

edge. These observations, and the ones described below, were made using a light microscope mounted on a load frame in such a way that observations of the edge of the specimen could be made while load was being applied. Even the eight or ten ksi applied to these otherwise undeformed specimens seemed to make the cracks easier to detect. For the loaded specimens, described below, the application of a load during observation greatly enhanced the visibility of cracks. Generally, loads somewhat below those used to create damage during the test were used during microscope observations. Some of the initial cracks observed in the undeformed specimen were not oriented transverse to the longitudinal (load) axis. Most of the initial cracks were found within one centimeter or so from the tabs on the specimens, a possible indication of end effects.

A Type I specimen was loaded to a level of 18 ksi (124 MPa) quasi-statically and sectioned. This stress level was thought to be close to the damage threshold as discussed earlier. A scanning electron microscope was used to examine the edges of one of the specimen halves. Transverse cracks were found in the 90° plies on the edges which were in the interior of the specimen, but none were found on the outside edges. However, the number of cracks found were not significantly larger than the number found in the undeformed specimen.

A very similar type of test was performed on another Type I specimen, wherein the same stress level was applied cyclically at 10 Hz (with $R=0.1$ for eight hundred and fifty thousand cycles. The number of transverse cracks observed on one outside edge was thirty six, while only twenty were found on the other, indicating that the specimen had been stressed more highly on one edge than the other. The edge which had sustained more damage was also delaminated. Although we did not have strain gages on this specimen, earlier tests indicated that a

difference of ten or twelve percent in the measured strain. Such a small difference would not account for the difference between the twenty ksi at which delamination was observed in this test and the forty (or more) ksi at which delamination was observed in static tests. It would appear, then, that fatigue loading caused more damage than static loading to the same level. We cannot say that more cracks were initiated, because we cannot be certain that small cracks did not initiate under static loading that were not found. However, it can be said that either more cracks are initiated or cracks grow larger (or both) under fatigue loading than under static loading to the same level. It should be noted that the time under load was different for the fatigue and static tests. The interior edges formed by the centerline section, had a somewhat larger number of cracks than the outer edge which did not delaminate. There are two ways such a result could occur. It could be caused by crack initiation in the interior of the specimen with subsequent growth to the edges. Alternatively, it could be caused by crack initiation at the edges with growth across the specimen width so that the center or interior region would be populated by cracks originating on both edges some of which had not reached the opposing edge. A comparison with the static test at this load also indicated a higher incidence of delamination than was observed for static loading. The motivation for these attempts to establish that the origin of cracks is in the interior or at the edge of the specimen is a desire to determine the nature and overall severity of the stress state in those two positions. While analytical determinations of those stress states are possible, their fidelity to reality is somewhat less than absolute, especially at the specimen edge. Moreover, the relationship of the stress states in those positions to the propensity

for failure is still incompletely understood so that experimental data is essential at this point.

A quasi-static loading of a Type I specimen to 30 ksi (206.8 MPa) was also investigated. The number of transverse cracks in the 90° plies that could be found using the light microscope with the specimen under load was essentially the same on the outside edges as on the edges from the interior of the specimen created by sectioning. Although it could not be established whether the same cracks appeared on the two (original) outside edges, the data supports the possibility that cracks which had formed extended across the specimen width at this stress level. From the standpoint of the effectiveness of experimental methods, it should be mentioned that transverse cracks in the 30° plies seemed to be more easily identified using a light microscope (at 100X) with the specimen under load than with a scanning electron microscope (SEM) at any magnification observing an unloaded specimen. On the other hand, cracks in the 45° layers seemed to be more easily found with the SEM than with the light microscope observing a loaded specimen.

A Type II specimen cyclically loaded at a stress amplitude of 20 ksi (137.8 MPa) for eight hundred fifty thousand cycles, like the Type I counterpart, showed more transverse cracks in the 90° plies than the specimens loaded quasi-statically to that level. In this case, however, significantly more cracks were found in the interior region than at the outer edges, again suggesting that crack growth from the edges or from the interior was occurring. It was also noticed that the cracks in the 45° plies were more prominent on the interior edges than on the outer edges.

In general, it would appear, based on our data to date, that damage

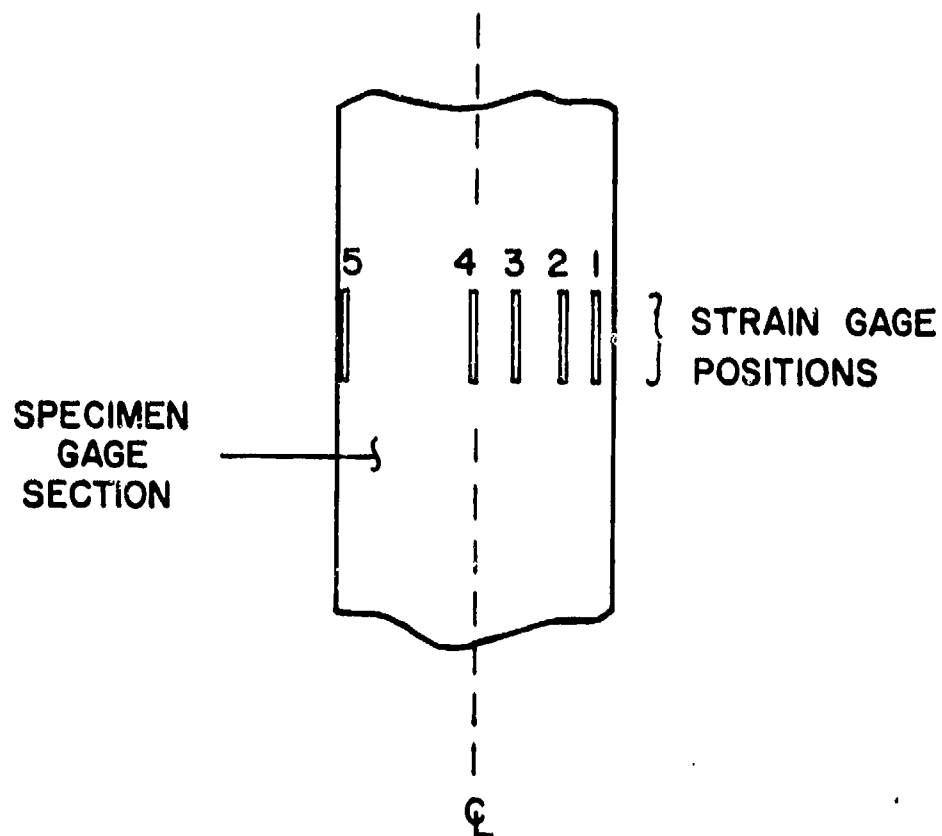


Figure 15. Strain gage positions on specimen gage setion

can be initiated in the form of transverse cracks in the 90° plies at 18-20 ksi (124-138 MPa), that cycled loading at a given stress level causes damage growth and may initiate new damage in the form of ply interface delamination, and that transverse cracks initiate either at the edge or interior and grow across the width (as well as through the thickness) with additional cyclic loading at a given stress or with elevated quasi-static loading. While these observations are supported by a relatively small number of test data at this point, no counter-examples were found. Investigations of this type are continuing.

8. Strain Gage Data

Strain gages were frequently used to monitor the deformation of the specimens during testing. Some of the positions of the gages used are shown schematically in Fig. 15. Since the transverse cracks that develop in the 90° plies are thought to initiate at the center or edge and then grow in the transverse plane, one of the objectives of the strain gage study was to detect any difference in the strain at those two positions which might provide an indication of how the cracks were growing. Variations between gage positions one and five, and the centerline position, four, were observed, with magnitudes up to about twelve percent. However, careful checking revealed that the observed differences were due to such things as variations in tab thickness, imprecise alignment of grip faces by the grip manufacturer, or non-uniform grip purchase. When all possible precautions were taken to avoid such external influences, the strain in all of the gages was essentially identical up to fracture, even when the actual fracture path passed through the gages themselves. When the strain at the gage one position for example, was higher than that at the gage five position

throughout the test, (which occurred on occasion) the final fracture initiated on the high strain side in the instances we were able to follow. However, no information concerning the initiation or growth of defects was obtained from these studies. We did learn that extreme care in the testing of these materials is essential, and that such things as camera lights could influence the strain gage readings significantly due to temperature changes of very small magnitude.

SECTION IV

PRINCIPAL FINDINGS & CONCLUSIONS

The present investigation has produced the following understandings and information.

1. Defect initiation, growth, and final fracture stages have been identified in these laminates. Initiation consists of transverse crack development in the 90° plies with crack surfaces essentially transverse to the load axis. At the time of first observation, these cracks usually extend through the thickness of a given 90° ply. Growth of these cracks with increasing load occurs in both directions transverse to the load axis, i.e., the transverse cracks grow through the laminate thickness into other layers and across the specimen width in the 90° ply or plies. Our understanding of the across-the-width growth is still incomplete. When growth spreads into the 0° plies final fracture occurs. The initiation and growth stages occur concurrently over a large part of the damage process. The density of transverse cracks continues to increase up to within about 15 percent of the fracture stress. Growth occurs over the last half to two thirds of the range of stress which causes failure.

2. Delamination does occur in these quasi-isotropic laminates if the 90° plies are grouped in the center of the laminate (Type I material). Delamination is predicted, in that case, by the analysis of Pagano and Pipes (3). When the 90° plies are the first underlayer (Type II material), delamination does not occur except immediately adjacent to the tab region in some cases.

3. The stress-strain response of these materials under quasi-static loading is essentially bilinear with the change in stiffness being caused by transverse crack formation in the 90° plies. However, in the case of the Type II material with a stacking sequence of $[0^\circ, 90^\circ, \pm 45^\circ]_s$, the change in stiffness is so gradual so as to make the assignment of a specific stress level to the so-called "knee" in the stress-strain curve highly discretionary. This continuous change in stiffness is caused by continuous initiation and growth of cracks in the 90° plies over a large load range, until a "saturation" spacing of cracks is reached. The stiffness change can be accurately predicted by laminate theory.

4. Cracks have been observed to initiate in the 90° plies at stress levels as low as 20 ksi. First ply failure is predicted by laminate theory failure criterions at that stress level if thermal residual stresses are included in the calculations. When a knee in the stress-strain curve is observed, it usually occurs between 35-40 ksi.

5. The Type I and Type II stacking sequences appear to cause the following differences in response:

- a. the strength of the Type II laminate is somewhat greater than that of the Type I laminates,
- b. the knee in the quasi-static loading stress-strain curve is more pronounced for Type I material than for Type II,

- c. delamination occurs in Type I material but not in Type II, and
- d. transverse cracks form in the two adjacent 90° plies in Type I material and are, therefore, larger and more well developed at a given load than their counterparts in the Type II material. Possibly because of their size, a larger number of transverse cracks were found at low load levels (close to the initiation threshold) in the Type I material than for the Type II material.

6. Cyclic loading causes additional flaw growth compared to static loading to an identical load level. The basic nature of the damage induced is essentially the same for static and dynamic loading, except for the enhancement of interlaminar cracking in the case of cyclic load application.

7. Defect growth has been observed during periods when the cross-head of a screw-type testing machine was held at a constant position, i.e., under constant elongation conditions. In those instances the load required to sustain that elongation dropped. In several instances, when the crosshead was stopped at a load quite close to the fracture load, delayed fracture occurred several seconds after the crosshead was stopped.

8. A number of investigative methods have proven to be very useful for the investigation of defects in these materials. They include light microscope examinations under load, scanning electron microscope studies, acoustic emission and ultrasonic attenuation measurements, video thermo-

graphy observations, and surface replication techniques. Of these methods, ultrasonic attenuation and/or diffraction appears to be the most precise, consistent, and reproducible indication of damage initiation and growth. It correlates best with actual defect observations, and shows changes which are much larger and more easily detected than the comparatively small and imprecise indications offered by a knee in the stress-strain curve, for example, in these materials.

As is frequently the case, the above findings have raised almost as many questions as they have answered. Our understanding of load history effects is quite incomplete. Although we have seen evidence, cited above, that quasi-static loading, cyclic dynamic loading and step loading produce certain distinctive features, no systematic explanation (or description) has been established for these effects. The differences in the response of quasi-isotropic laminates having different stacking sequences is also incompletely investigated. In fact, these differences raise a general question concerning the limits of laminate theory for the analysis or description of damage states in these materials. It is also fairly obvious that the constraint effects on damage development in a given ply exerted by adjacent plies is a general problem which has been rather badly neglected and which must be addressed if some of our findings are to be properly understood. Finally, how and where cracks start is still a partial mystery. It is not known how manufacturing defects are involved in initiation, if at all, and it has not been established firmly that edges are exclusive damage initiators. These and other items require further investigative attention.

REFERENCES

1. Reifsnider, K. L., Henneke, E. G., and Stinchcomb, W. W., "Defect-Property Relationships in Composite Materials", AFML-TR-76-81, April 1976.
2. Stinchcomb, W. W., Henneke, E. G., and Hayford, D. T., "Short Beam Shear Tests of Polymeric Laminates and Unidirectional Composites," Semi-Annual Report, NASA Grant NSG-1254, 1 April 1976 - 30 September, 1976.
3. Renieri, G. D. and Herakovich, C. T., "Nonlinear Analysis of Laminated Fibrous Composites," VPI&SU, College of Engineering Report VPI-E-76-10, June, 1976.
4. Pagano, N. J. and Pipes, R. B., "Some Observations on the Interlaminar Strength of Composite Materials," Int. J. of Mech. Sci., Vol. 15 (1973).